

Smoldering Ignition by Concentrated Irradiation Spot

Ms. Siyan Wang 王思言

Research Centre for Fire Safety Engineering, The Hong Kong Polytechnic University

Abstract

Spotting ignition is a common ignition phenomenon for indoor compartment fire and outdoor wildland fire, but little research has quantified its characteristics. Herein, we study the smoldering ignition of tissue paper by concentrated sunlight spots up to 780 kW/m^2 , which are focused by a transparent glass sphere. The diameter of the sunlight spot on the targeted paper ranges from 1.5 mm to 20.0 mm by varying the position of the paper within the focal length. Given a size of the irradiation spot, the smoldering ignition time decreases as the irradiation increases, follows the classical piloted flaming ignition theory. However, the measured minimum spot irradiation for smoldering ignition is not constant but much higher than 11 kW/m^2 from the cone-calorimeter test. As the diameter of the irradiation spot decreases from 20.0 mm to 1.5 mm, the minimum irradiation for smoldering ignition increases from 17.5 kW/m^2 to 205 kW/m^2 , and the ignition energy increases from 0.084 MJ/m^2 to 2.0 MJ/m^2 . A simplified heat transfer analysis reveals that the radial conductive cooling effect within the fuel becomes more dominant for smaller spotting areas. This work quantifies the fire risk of the concentrated light spot and helps understand the mechanism of spotting smoldering ignition.

Keywords: Smoldering ignition, Critical ignition heat flux, Ignition energy

1. Introduction

The ignition of combustible materials plays a central role in the initiation and growth of devastating fire events. Many ignition events in structure and wildland fires occur remotely by a point heating source [1], such as the firebrands [2–4], hot metal particles [4,5], dripping [6], laser [7,8], lightning strike [9], and concentrated irradiation [10–13]. There are also frequent fire accidents worldwide initiated by the concentrated sunlight spot, which is reflected by the curved mirror or focused by dew droplet, curved glass window and decorations, transparent fish bowls and cylindrical bottles filled with water in residential buildings and wildland [14–16]. From 2010 to 2015, 125 fires in the UK triggered by the concentrated sunlight spot were reported [17], posing severe threats to human lives and properties. However, to the best of authors' knowledge, such a remote ignition phenomenon has been rarely studied quantitatively, bringing a primary knowledge gap.

Over the past 50 years, only limited studies have investigated the flaming ignition by a laser spot or concentrated irradiation. Kashiwagi [7,8] showed that the minimum radiant heat fluxes of flaming auto-ignition are 90 kW/m^2 for red oak and 160 kW/m^2 for PMMA with a laser spot diameter of 2–3 cm. Grishin et al. [10] generated a light beam by a tungsten lamp to ignite the porous forest fuel layer with a bulk density of $6\text{--}24 \text{ kg/m}^3$ and revealed that the required irradiant heat flux for flaming ignition decreases as the heating diameter increases from 8 mm to 27 mm. Warren [11] concentrated sunlight by a spherical water-filled glass bowl with a diameter of 200 mm and demonstrated the possibility of smoldering ignition of print paper by concentrated irradiation.

Compared to the spotting ignition by the direct contact of hot metal spark and firebrands (i.e., transfer of heat source and fuel) [2,4], the ignition by concentrated irradiation spot only involves energy transfer. Thus, such an ignition process is simpler, which can also provide valuable information to other

spotting ignition processes. Once an intense irradiation spot is applied, the fuel can be heated, dried, decomposed, and then smolder. Smoldering combustion is slow, low-temperature and flameless burning of porous fuel, which is sustained as a heterogeneous oxidative process and different from the flaming combustion [20]. It is also a common fire phenomenon in both structures and wildland, such as the burning of upholstered furniture, mattresses, firebrand, litter layer, and peatlands [21,22]. Therefore, to fully understand smoldering ignition is important, but so far, little research has studied the smoldering ignition by a point heat source, and the ignition criteria are still poorly understood.

This work investigated the smoldering ignition of the multiple-layer tissue paper by an intense point irradiation, i.e., the sunlight spot concentrated by a spherical glass ball. Within the focus length, the diameter of heating spot was varied from 1.5 mm to 20 mm, and the intensity of irradiation was varied up to 780 kW/m². The ignition delay time, critical heat flux, and ignition energy of smoldering by the irradiation spot were quantified. Finally, a simplified heat transfer model is proposed to (1) explain the varying minimum irradiation and energy for smoldering ignition and (2) quantify the potential ignition risk initiated by the concentrated sunlight in structure and wildland fires.

2. Experimental methods

2.1. Materials and apparatus

Thin tissue paper made of unbleached pulp was used in the experiment, as it was typical thin fuel in the residential buildings and wildland left by humans. Before the test, the tissue paper was first oven-dried at 75 °C for 48 h, and its dried bulk density was measured to be 98 kg/m³. Afterwards, it was placed into an electronic dry cabinet to avoid the re-absorbing of moisture from the air. For the test, the tissue was first cut into a size of 60 mm × 60 mm, and six layers of tissue were packed into a sample with an overall thickness (δ) of about 2 mm (see Fig. 1). For a single layer of tissue (about 0.1-mm thick), the concentrated irradiation spot would create a hole on the tissue directly without ignition, so the multiple layers of tissue were used.

In the experiment, the natural sunlight was concentrated by a 150-mm K9 crown glass sphere with a refractive index (n_c) around 1.53. The spherical lens minimized the operation of the concentrator during the experiment because its projection of sunlight beam was fixed and insensitive to the position of the sun. The focal length and back focal length of the crown glass sphere were theoretically calculated to be 108 mm and 33 mm [23]. A positioning device was fixed perpendicular to the surface of the base stand (Fig. 1). To ensure that the device was parallel to the sunlight, the angle of the base stand was adjusted until the light beam passed through the hole in the middle of the front aluminum block and projected on the middle of the back aluminum block. A solar power meter was fixed at the front towards the sunlight direction to record real-time solar irradiation (\dot{q}_s''). The sample frame was a hollow box that provided a volume of 60 × 60 × 2 mm³ for the tissue sample and was inserted into the sample holder. The sample holder was installed on a slide which can adjust its distance between the tissue sample and the glass sphere with a precision of 0.5 mm.

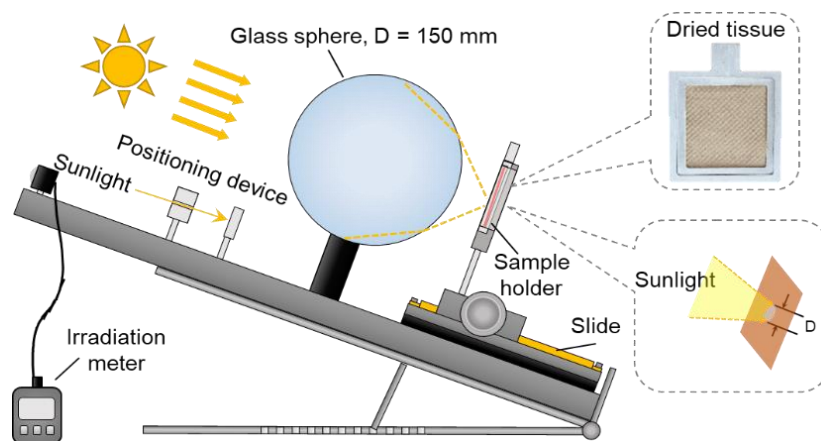


Fig. 1. The schematic diagram of the designed experiment apparatus.

2.2. Irradiant heat flux of light spot

Traditionally, the value of irradiant heat flux can be measured by a radiometer. However, as the diameter of light spot decreases, the heat flux of sunlight concentrated by the glass sphere could exceed 500 kW/m², which was much higher than the upper limit (usually 100-200 kW/m²) of a conventional radiometer. Thus, to quantify the high irradiation of concentrated sunlight spot, the optical simulation by *TracePro* was first used to correlate the size of the light spot and theoretical irradiation (\dot{q}_c'') concentrated by a 150-mm crown glass sphere.

In the optical simulation, the overall concentration factor (C) considered not only the optical concentration, but also the actual energy dissipation, such as the light reflected, refracted and absorbed by the glass sphere in the transmitting process [11]. The peak concentration factor is about 900 at about $D = 2$ mm, which is not at the optical back focal length. Due to the loss resulted by the reflection, refraction and spherical aberration, the concentration factor of the minimum light spot ($D = 1.5$ mm) is about 460 at the back focal length. With the instant solar irradiation (\dot{q}_s'') and the concentration factor for different light spots, the actual concentrated solar irradiation heat flux can be calculated as

$$\dot{q}_c'' = C\dot{q}_s'' \quad (1)$$

For example, if the solar irradiation is 1 kW/m² [24], the resultant heat flux peaks at around 900 kW/m², which is close to the literature value [11].

Sunlight through the glass sphere will form a caustic zone instead of a focal point due to the existence of spherical aberration, that is, the blurry appearance of the outer part of the view of a convex lens [25]. As the spots become intensively blurry beyond the focus length, their edge could be hardly identified. Therefore, to maintain a better precision, only light spots within the back focal length with clearly defined boundary were adopted in the experiment [25]. In total, four different positions (x) of 3 mm, 13 mm, 19 mm, and 33 mm within the glass sphere's back focal length were tested, with respect to four heating diameters (D) of 20.0 mm, 9.0 mm, 5.5 mm, and 1.5 mm, as summarized in Table 1.

Table 1. Summary of diameters of irradiation spots (D) and concentration factors (C) at different distances from the sphere.

Distance from sphere, x (mm)	33.0	19.0	13.0	3.0
Irradiation spot diameter, D (mm)	1.5	5.5	9.0	20
Concentration factor, C	460	294	134	38

2.3. Experimental procedures

Before the test, the diameter of light spot was adjusted by controlling the distance between the glass sphere and sample. Afterwards, the light spot was shielded by a piece of black cardboard, and the tissue sample was inserted into the sample holder. Once the instant solar irradiation heat flux (\dot{q}_s'') read by the solar power meter was relatively stable, the back cardboard was removed to allow the light spot to apply on the fuel surface. Then, the sample was heated by the light spot for a prescribed duration (t).

For a flaming ignition, the ignition can be judged by the appearance of a flame. However, it was not possible to instantaneously determine the success of smoldering ignition and the exact ignition time. Thus, after heating, the tissue sample was left in the controlled environment without wind for another 5 min for further observation. The successful smoldering ignition was defined, if the smoldering spot successfully propagated outwards from the heating region within 5 min and eventually burned out the sample. If no smoldering ignition occurred, the heating duration was increased until the ignition was successful. Then, more than 100 tests were conducted under the same heating diameter with a range of concentrated irradiations. Afterwards, the diameter of the heating spot was varied by moving the sample within the focal length to investigate its effect on the smoldering ignition.

Totally, more than 600 tests were conducted outdoor on typical summer sunny days with a blue sky. Depending on the weather and solar zenith angle, the instant solar radiation ranged from 0.2 kW/m²

(at nightfall) to 1.6 kWm^2 (at noon). During the test, the ambient temperature was $29 \pm 2 \text{ }^\circ\text{C}$, the relative humidity was $82 \pm 10 \%$, the wind speed was $5.5 \pm 0.9 \text{ m/s}$, and the ambient pressure was 101 kPa .

3. Results and discussion

3.1. Smoldering spotting ignition phenomena

Fig. 2a shows an example of a successful smoldering ignition by the concentrated irradiation spot with a diameter of 1.5 mm and a resultant irradiation heat flux of 560 kW/m^2 . Once the irradiation spot was applied on the sample surface, some smoke was released. Continuing the heating, the surface layer within the light spot turned black and broke that allowed the light beam to heat the lower layer directly. After heated for about 8 s , the sample was detached from the apparatus and left in the controlled environment (without wind) for another 5 min . As a result, the black spot expanded outwards evenly with a stable rate and eventually burned out the sample. Fig. 2b shows an example of a failed smoldering ignition by the concentrated irradiation spot with a diameter of 1.5 mm and a resultant radiant heat flux of 300 kW/m^2 . Initially, smoke and a charring tendency was also observed. However, after heating for 8 s , no smoldering propagation phenomenon was observed, indicating a failed ignition.

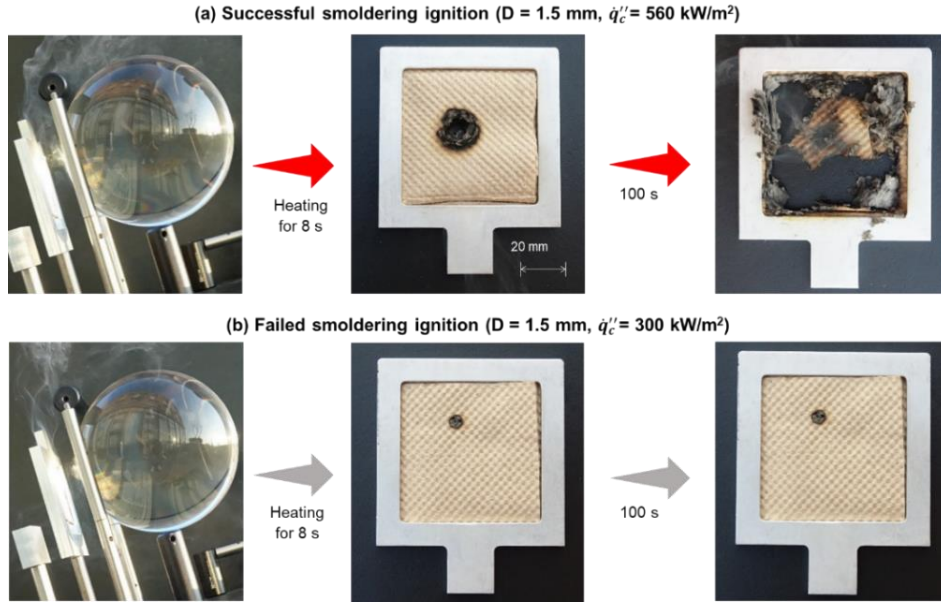


Fig. 2. Smoldering ignition of dried tissue samples by concentrated irradiation spot with a diameter of 1.5 mm for 8 s , (a) successful ignition under irradiation of 560 kW/m^2 , and (b) failed ignition under irradiation of 300 kW/m^2 .

3.2. Irradiation duration for ignition and critical irradiation

The experimental outcomes under different diameters of concentrated irradiation spots (D) and the resultant irradiant heat fluxes (\dot{q}_c'') are summarized in Fig. 3, where the solid and hollow markers represent failed and successful ignition, respectively. Note that the instant solar radiation (\dot{q}_s'') changed from time to time, so there was a large scattering in the irradiation value. Given the diameter of the concentrated irradiation spot, the required heating duration for the smoldering ignition (t_{ig}) decreases as the external irradiation increases. This trend is similar to the piloted flaming ignition theory, where the flaming ignition time is mainly the required heating time for pyrolysis [26]. In general, the required duration for smoldering ignition (t_{ig}) is the time to heat the fuel surface to a critical smoldering temperature (T_{sm}) which is the threshold temperature of char oxidation. For a typical 1-D thermally-thin material ($Bi < 0.1$), if heat transfer inside the fuel is neglected, the ignition time can be approximated as

$$t_{ig} \approx \frac{\rho c_p \delta (T_{sm} - T_0)}{\dot{q}_c'' - \dot{q}_{crt}''} \quad (2)$$

where ρ , c_p , and δ are the density, specific heat, and thickness of fuel, respectively; T_0 is the initial fuel temperature; and \dot{q}''_{crt} is the critical heat flux for smoldering ignition.

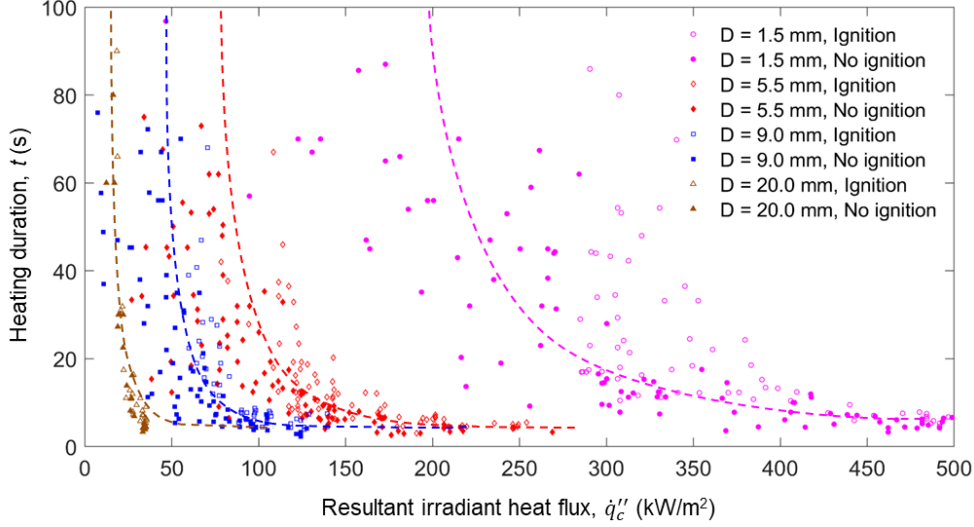


Fig. 3. The experimental outcomes under different diameters of irradiation spots (D) and the resultant irradiant heat fluxes (\dot{q}''_c), where the solid and hollow markers represent failed and successful ignition, respectively.

Fig. 4 further verifies the relationships between t^{-1} and \dot{q}''_c with different diameters of the concentrated irradiation spots, where the linear correlations of the ignition boundaries (i.e., t_{ig}) were obtained from the logistic regression model [27]. Based on Eq. (2), the critical heat flux for smoldering ignition (\dot{q}''_{crt}) can be estimated by a linear extrapolation of ignition boundary towards the x axis (i.e., $t_{ig} \rightarrow \infty$), as indicated in Fig. 4. Interestingly, as the diameter of concentrated irradiation spot decreases from 20 mm to 1.5 mm, the critical heat flux increases dramatically from 18 kW/m² to 205 kW/m² (see the summary in Table 2).

The critical irradiation for the smoldering ignition of tissue sample under the cone calorimeter is also shown in Fig. 5, where the 100-mm heating diameter of the cone that can fully cover the whole surface of 60 mm × 60 mm tissue sample (i.e., $D = 60$ mm). Furthermore, the critical heat fluxes for flaming auto-ignition of PMMA (square) and red oak wood (diamond) by a laser spot [7] and loosely pine needle bed by a light beam (triangle) [10] are also plotted for references. Clearly, as the diameter of the irradiation spot increases, the critical heat flux for smoldering ignition decreases, and eventually, it approaches a near-minimum value obtained from the cone calorimeter (about 11 kW/m²). An empirical correlation between the critical heat flux (\dot{q}''_{crt}) for smoldering ignition and the diameter of concentrated irradiation spot (D) can be formulated as

$$\dot{q}''_{crt} = \frac{300}{D} + 11 \quad (3)$$

where common units of [kW/m²] for \dot{q}''_{crt} and [mm] for D are used. The excellent linearity is found in the logarithm coordinate in Fig. 5a.

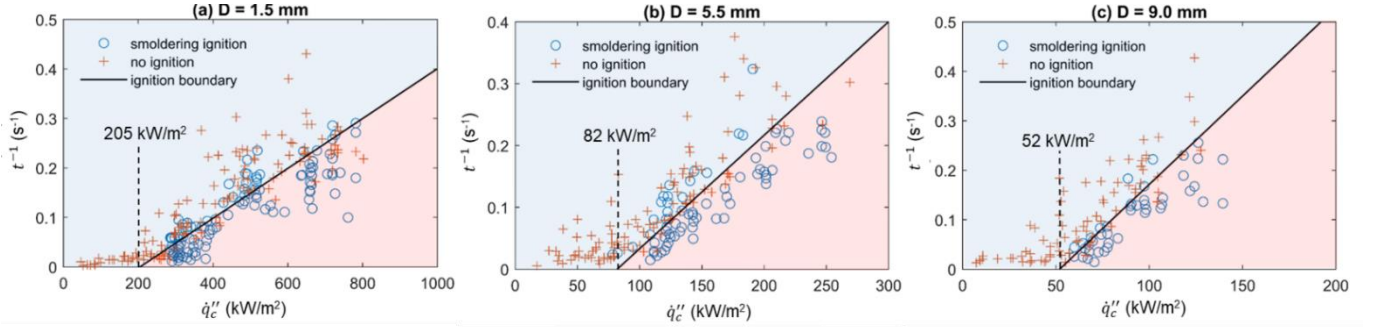


Fig. 4. The relationship between t^{-1} and \dot{q}''_c under different spot diameters and the critical irradiation levels, where the fitting curves of ignition boundaries were obtained from the logistic regression model.

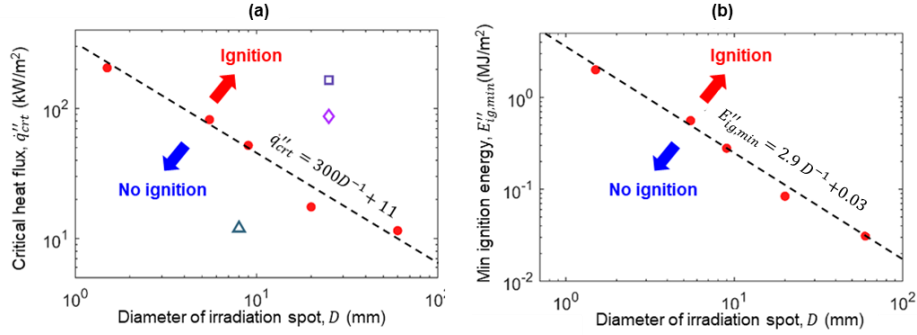


Fig. 5. The relationship between diameters of irradiation spots (D) and (a) critical ignition heat fluxes (\dot{q}''_{crt}); and (b) smoldering ignition energy ($E''_{ig,min}$).

Table 2. Summary of critical heat flux (\dot{q}''_{crt}) and minimum ignition energy ($E''_{ig,min}$) for smoldering spotting ignition with different light spot diameters.

Irradiation spot diameter, D (mm)	1.5	5.5	9.0	20	60*
Critical irradiation for ignition, $\dot{q}''_{c,crt}$ (kW/m ²)	205	82	52	17.5	11.5
Minimum ignition energy, $E''_{ig,min}$ (MJ/m ²)	2.0	0.56	0.28	0.084	0.031

*The whole 60 mm × 60 mm sample was tested under the irradiation of the cone calorimeter.

3.3. Ignition energy

The total smoldering ignition energy (E''_{ig}) for the thin tissue sample provided by the concentrated irradiation can be approximately calculated as

$$E''_{ig} = \dot{q}''_c t_{ig} \approx \rho c_p \delta (T_{sm} - T_0) \frac{\dot{q}''_c}{\dot{q}''_c - \dot{q}''_{crt}} \quad (4)$$

where the minimum heating duration for ignition (t_{ig}) given an irradiation heat flux (\dot{q}''_c) could be obtained from Fig. 4. The smoldering ignition energy by different diameters of the irradiation spot is shown in Fig. 6. As the irradiation level (\dot{q}''_c) increases, the ignition energy gradually decreases and eventually approaches a minimum value, as shown in Fig. 6. Then, the minimum ignition energy of smoldering ($E''_{ig,min}$) can be defined. Eq. (4) suggests that $E''_{ig,min}$ should be a material constant of $\rho c_p \delta (T_{sm} - T_0)$ at $\dot{q}''_c \gg \dot{q}''_{crt}$, which disagrees with the different trendlines in Fig. 6.

Fig. 5b further compares the values of $E''_{ig,min}$ for different spot diameters (also see Table 2). As the diameter of irradiation spot increases from 1.5 mm to 20 mm, the $E''_{ig,min}$ decreases from 2.0 MJ/m² to 0.084 MJ/m². An empirical correlation between minimum ignition energy ($E''_{ig,min}$) and spot diameter (D) can be found as

$$E''_{ig,min} = \frac{2.9}{D} + 0.03 \quad (5)$$

where common units of $[\text{MJ}/\text{m}^2]$ for $E''_{ig,min}$ and $[\text{mm}]$ for D are used. The excellent fitting (R^2 coefficient of 0.99) can be found in the logarithm coordinate in Fig. 5b. In other words, both the critical irradiation heat flux and the minimum ignition energy change with the diameter of irradiation spot, indicating that the conventional 1-D heat transfer analysis becomes invalid for irradiation spot smaller than 20 mm, even if the fuel is thin.

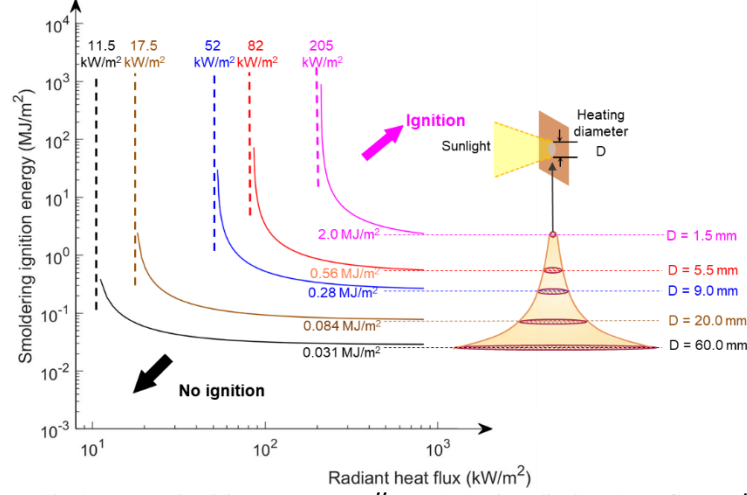


Fig. 6. The relationship between ignition energy (E''_{ig}) and the irradiation heat flux (q''_c) with different diameters of the irradiation spot (D), where the minimum ignition energy ($E''_{ig,min}$) could be represented as the dashed trendline.

3.4. Theoretical analysis

To scientifically understand the effect of light spot diameter on the critical heat flux of smoldering ignition, a minimum smoldering ignition temperature $T_{ig,s} \approx 250 \text{ }^\circ\text{C}$ is defined [28]. Then, a simplified calculation based on thermal equilibrium is proposed to a heating spot on the sample, as shown in Fig. 7.

By definition, considering a 3-D cooling effect, the critical heat flux for ignition should balance environmental heat loss (\dot{q}''_{∞}) and internal conductive heat loss to the virgin fuel (\dot{q}''_{cond}) [29] as

$$\frac{\pi D^2 \dot{q}''_{c,crt}}{4} = \frac{\pi D^2 \dot{q}''_{\infty}}{2} + \pi D \delta \dot{q}''_{cond} \quad (6)$$

which can be further expressed and simplified as

$$\dot{q}''_{c,crt} = 2\dot{q}''_{\infty} + \frac{4\delta \dot{q}''_{cond}}{D} \quad (7)$$

where δ is the sample thickness. Therefore, as the heating diameter increases, the critical heat flux for ignition decreases, agreeing with the trend in Fig. 5a. For a small heating diameter, the internal conductive heat loss will dominate, thus the relationship between $\dot{q}''_{c,crt}$ and D can be approximated as

$$\dot{q}''_{c,crt} \propto \frac{1}{D} \quad (\text{small light spot}) \quad (8)$$

As the heating diameter (D) further increases, the second part of Eq. 6 gradually approaches to zero, and the internal conduction becomes negligible. Therefore, for a larger heating diameter, the heat transfer can be approximated as a 1-D process, and the critical heat flux for smoldering ignition can be calculated as

$$\dot{q}''_{c,crt} = 2\dot{q}''_{\infty} = 2\varepsilon\sigma(T_{ig,s}^4 - T_{\infty}^4) + 2h_{conv}(T_{ig,s} - T_{\infty}) \quad (\text{large heating diameter}) \quad (9)$$

where $\varepsilon = 0.9$ is the emissivity of tissue paper, $\sigma = 5.67 \times 10^{-8} \text{ Jm}^{-2}\text{s}^{-1}\text{K}^{-4}$ is the Stefan-Boltzmann constant, T_{∞} is the ambient temperature and h_{conv} is the free-convection heat transfer coefficient [29]. For a horizontal hot plate, h_{conv} can be estimated from an empirical correlation [30] as

$$h_{conv} = 1.52(T_{ig,s} - T_{\infty})^{\frac{1}{3}} \quad (10)$$

Then, for a large heating diameter, the critical heat flux for smoldering ignition can be calculated as 11.5 kW/m^2 , which successfully explains the experimental measurement under a large heating diameter.

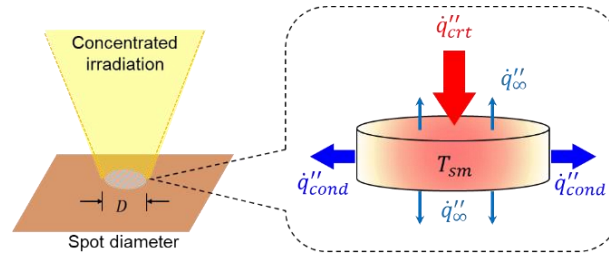


Fig. 7 Schematic diagram of smoldering ignition by concentration irradiation spot, where the critical heat flux for ignition should balance environmental heat loss (\dot{q}''_{∞}) and internal conductive heat loss from the perimeter (\dot{q}''_{cond}).

Conclusions

In this work, we investigated the smoldering ignition of the multiple-layer thin tissue paper by tiny irradiation spots. The irradiant spot was generated via concentrating sunlight by a transparent glass sphere with a diameter of 150 mm and a focal length of 108 mm. To quantify the concentrated radiant heat flux, optical simulation by *TracePro* was conducted to model the diameter of irradiation spot and radiation distribution. We found that as the solar irradiation increases or the diameter of irradiation spot decreases, the resultant irradiance increases. Given a size of irradiation spot, the smoldering ignition time decreases as the concentrated irradiation increases, following the classical piloted ignition theory. However, the measured minimum spot irradiation for smoldering ignition is not constant but much higher than 11 kW/m^2 measured from the cone-calorimeter test. As the diameter of irradiation spots decreases from 20.0 mm to 1.5 mm, the minimum irradiation for smoldering ignition increases from 17.5 kW/m^2 to 205 kW/m^2 , and the ignition energy increases from 0.084 MJ/m^2 to 2.0 MJ/m^2 .

A simplified heat transfer analysis was proposed, which successfully highlights the 2-D cooling effect on the limiting condition for ignition by tiny irradiation spot. Future numerical simulations are needed to reveal the underlying physical and chemical process of smoldering spotting ignition.

References

- [1] Caton SE, Hakes RSP, Gollner MJ. Review of Pathways for Building Fire Spread in the Wildland Urban Interface Part I: Exposure Conditions. *Fire Technology* 2017;53:429–73. doi:10.1007/s10694-016-0589-z.
- [2] Fernandez-Pello AC. Wildland fire spot ignition by sparks and firebrands. *Fire Safety Journal* 2017;91:2–10. doi:10.1016/j.firesaf.2017.04.040.
- [3] Manzello SL, Suzuki S, Gollner MJ, Fernandez-Pello AC. Role of firebrand combustion in large outdoor fire spread. *Progress in Energy and Combustion Science* 2020;76:100801. doi:10.1016/j.peccs.2019.100801.
- [4] Wang S, Huang X, Chen H, Liu N. Interaction between flaming and smoldering in hot-particle ignition of forest fuels and effects of moisture and wind. *International Journal of Wildland Fire* 2017;26:71–81. doi:10.1071/WF16096.
- [5] Urban JL, Zak CD, Fernandez-Pello C. Cellulose spot fire ignition by hot metal particles. *Proceedings of the Combustion Institute* 2015;35:2707–14. doi:10.1016/j.proci.2014.05.081.

- [6] Sun P, Lin S, Huang X. Ignition of thin fuel by thermoplastic drips: An experimental study for the dripping ignition theory. *Fire Safety Journal* 2020;115:103006. doi:10.1016/j.firesaf.2020.103006.
- [7] Kashiwagi T. Experimental observation of radiative ignition mechanisms. *Combustion and Flame* 1979;34:231–44. doi:10.1016/0010-2180(79)90098-1.
- [8] Kashiwagi T. Effects of sample orientation on radiative ignition. *Combustion and Flame* 1982;44:223–45. doi:10.1016/0010-2180(82)90075-X.
- [9] Zhang H, Qiao Y, Chen H, Liu N, Zhang L, Xie X. Experimental study on flaming ignition of pine needles by simulated lightning discharge. *Fire Safety Journal* 2020:103029. doi:10.1016/j.firesaf.2020.103029.
- [10] Grishin AM, Golovanov AN, Medvedev V V. On the ignition of a layer of combustible forest materials by light radiation. *Combustion, Explosion and Shock Waves* 1999;35:618–21. doi:10.1007/BF02674534.
- [11] Warren DW. Optical Modeling of Fire Hazards Arising from Sunlight Focused by Water. *Fire Technology* 2014;50:1327–34. doi:10.1007/s10694-013-0353-6.
- [12] Engerer JD, Brown AL, Christian JM. Ignition and damage thresholds of materials at extreme incident radiative heat flux. 2018 Joint Thermophysics and Heat Transfer Conference 2018:1–27. doi:10.2514/6.2018-3764.
- [13] Brown AL, Engerer JD, Ricks AJ, Christian J, Yellowhair J. Datasets for material ignition from high radiant flux. *Fire Safety Journal* 2020:103131. doi:10.1016/j.firesaf.2020.103131.
- [14] Goldstone BM. Hazards from the concentration of solar radiation by textured window glass. London: HMSO; 1982.
- [15] Dyke KS Van. The fish bowl as a fire hazard. *Science* 1937;86:122–3. doi:10.1126/science.86.2223.122-a.
- [16] Wildfire in Guilin caused by a plastic bottle. *Guilinlife* 2019.
- [17] Brigade step up sunlight warning after another refraction blaze. *London Fire Brigade* 2015.
- [20] Rein G. Smoldering Combustion. *SFPE Handbook of Fire Protection Engineering* 2014;2014:581–603. doi:10.1007/978-1-4939-2565-0_19.
- [21] Quintiere J. *Principles of Fire Behaviour*. New York: Alar Elken; 1997.
- [22] Lin S, Huang X. Quenching of smoldering: Effect of wall cooling on extinction. *Proceedings of the Combustion Institute* 2020;38. doi:10.1016/j.proci.2020.05.017.
- [23] *Springer Handbook of Lasers and Optics*. 2007. doi:10.1007/978-0-387-30420-5.
- [24] Kopp G, Lean JL. A new, lower value of total solar irradiance: Evidence and climate significance. *Geophysical Research Letters* 2011. doi:10.1029/2010GL045777.
- [25] Avendaño-Alejo M, Castañeda L, Moreno I. Properties of caustics produced by a positive lens: meridional rays. *Journal of the Optical Society of America A* 2010. doi:10.1364/josaa.27.002252.
- [26] Lin S, Sun P, Huang X. Can peat soil support a flaming wildfire? *International Journal of Wildland Fire* 2019;28:601–13. doi:10.1071/wf19018.
- [27] Hosmer DW, Lemeshow S, Sturdivant RX. *Applied Logistic Regression: Third Edition*. 2013. doi:10.1002/9781118548387.
- [28] Lin S, Huang X, Urban J, McAllister S, Fernandez-Pello C. Piloted ignition of cylindrical wildland fuels under irradiation. *Frontier in Mechanical Engineering* [under Review] 2019.
- [29] Lin S, Cheung YK, Xiao Y, Huang X. Can rain suppress smoldering peat fire? *Science of the Total Environment* 2020;727:138468. doi:10.1016/j.scitotenv.2020.138468.
- [30] Holman JP. *Heat Transfer*. 10th ed. New York: McGraw-Hill; 2008.

Acknowledgements

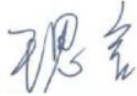
First and foremost, I would like to express my great and genuine gratitude to my supervisor, Dr. Xinyan Huang, Assistant Professor and Deputy Director, Research Centre for Fire Safety Engineering, The Hong Kong Polytechnic University, for giving me the precious opportunity to carry out this meaningful research and providing invaluable guidance throughout the progress. I was deeply inspired by his vision and motivation. Besides, I am extremely grateful to Mr. Shaorun Lin and Mr. Yanhui Liu who worked together with me to conduct experiments and theoretical analysis. My special thanks will also go to Dr.

Michael J. Gollner, Assistant Professor, University of California, Berkeley, for his keen interest shown in this work that helped me to complete it successfully.

This research is funded by the National Natural Science Foundation of China (NSFC) No. 51876183 and the Society of Fire Protection Engineers (SFPE) Educational & Scientific Foundation.

Disclaimer

I, Siyan Wang, certify that this paper is all my own work unless where referenced or acknowledged.

Handwritten signature in blue ink, appearing to be the Chinese characters '王思彦' (Wang Siyan).